Journal of Sol-Gel Science and Technology (2019) 89:486–491
https://doi.org/10.1007/s10971-018-4869-6

ORIGINAL PAPER: NANO-STRUCTURED MATERIALS (PARTICLES, FIBERS, COLLOIDS, COMPOSITES, ETC.)

# $NiCo_2O_4$ nanolayer cover on carbon cloth as anode materials for supercapacitors

Zhihong Deng[1,2] · Jianzhe Luo[1] · Linyu Yang[1] · Jun Liu[1,3] · Kunjie Zhu[1] · Jie Min[1] · Guoyou Wang[2]

Received: 16 July 2018 / Accepted: 29 October 2018 / Published online: 13 November 2018


## Abstract

$NiCo_2O_4$ nano-layer covered on surface of carbon cloth for high-performance supercapacitors is successfully fabricated by a one-step route which only involved a modified sol–gel method. The binder-free electrode only with simple layer covering on carbon cloth displays outstanding pseudocapacitive behaviors in 2 M KOH, which exhibits high specific capacitances of 944.5 F $g^{-1}$ at 1 A $g^{-1}$ and 702.4 F $g^{-1}$ at 20 A $g^{-1}$after activation, as well as excellent cycling stability. The specific capacitance can still retain 859.5 F $g^{-1}$ (91% retention) at a current density of 1 A $g^{-1}$ after 3500 cycles.

## Graphical Abstract

A uniform ultrathin active substance $NiCo_2O_4$ supercapacitor electrode was formed directly on carbon cloth by modified sol–gel method. This supercapacitor electrode has high specific capacity and excellent rate performance.

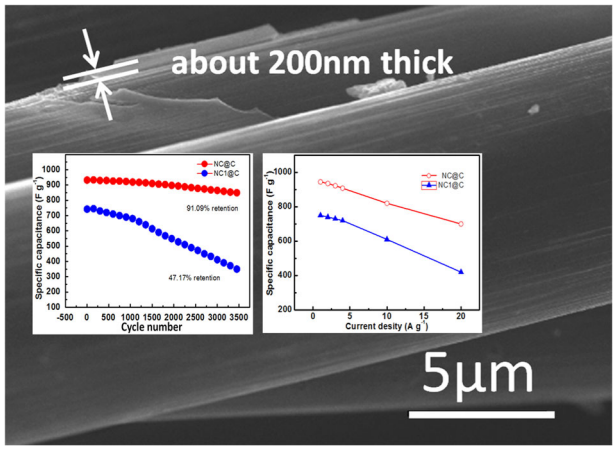


✉ Zhihong Deng
zhihongdeng@126.com

✉ Jun Liu
liujun4982004@csu.edu.cn

✉ Guoyou Wang
gywang04@163.com

[1] School of Materials Science and Engineering, Central South University, 410083 Changsha, Hunan, China

[2] College of Science, Hunan University of Technology, 412007 Zhuzhou, Hunan, China

[3] Education Ministry Key Laboratory of Non-ferrous Materials Science and Engineering, Central South University, 410083 Changsha, Hunan, China

**Highlights**

- In this paper, we report the synthesis of nanostructured $NiCo_2O_4$@carbon cloth (NC@C) electrodes by sol–gel method.
- The synthesis strategy involves a novel method:sol–gel method to fabricate binder-less electrode.
- The synthesized $NiCo_2O_4$ nano layer uniformly covered on the surface of carbon nanofibers.
- The synthesized $NiCo_2O_4$@carbon cloth electrode exhibits excellent electrochemical performance.

**Keywords** Supercapacitor · Sol–gel · $NiCo_2O_4$ · Binder-free

## 1 Introduction

The development of portable electronic devices, electric vehicles and many highly energy consumption application create generate enormous demand for electrochemical energy storage with higher power and energy densities [1–4]. Electrochemical capacitors, also called supercapacitors, attracted much attention due to its more excellent performance of high power density and good stability than that of the most widely used batteries, are probably the most important next-generation energy storage device [5–11]. According to the energy storage mechanism supercapacitor can be classified into two types which are electrical double-layer capacitors [12, 13] and faradic capacitors [14]. Among these two types, Faradic capacitors have much higher specific capacitance and energy density than those of electrical double-layer capacitors.

As a kind of energy storing device which can realize quick charge and discharge, Faradic capacitors are widely researched due to their high reliability,long lifespan and high power density [15, 16]. Transition metal oxides are reported to be a class of promising active materials for supercapacitors due to their multiple oxidation states [17–19]. Among them, $NiCo_2O_4$ has been suggested as a viable candidate at a low price, based on its high specific capacitance and fast Faradaic reactions. Compared to the single-component oxides, $NiCo_2O_4$ offer richer redox chemistry and combine the contributions from both Co and Ni ions [20, 21]. According to electrode structure, $NiCo_2O_4$ electrode can be classified into two basic types: binder and binder-free [22–26]. In the former case, the working electrode is prepared by the traditional slurry-coating technique for electrochemical measurement. In the latter case, electroactive $NiCo_2O_4$ nanostructures are directly deposited on conductive substrates used as binder-free electrodes for supercapacitors. The deposition method includes electrochemical deposition method and hydrothermal method. In this paper, we report the synthesis of nanostructured $NiCo_2O_4$@carbon cloth (NC@C) electrodes only by one-step sol–gel method. To the best of our knowledge, there have been no reports about sol–gel method to fabricate binder-less electrode in the literature by others.

## 2 Experimental

### 2.1 Preparation of samples

**Synthesis of NC@C Structure**. all chemicals including acetone, ethanol, citric acid, $Ni(NO_3)_2{\cdot}6H_2O$, and $Co(NO_3)_2{\cdot}H_2O$ from Sinopharm Chemical Reagent Co. were of analytical grade and used without any further purification. commercial carbon clothes (WOS 1002, CeTech, the thickness is 360 μm,$2 \times 1$ $cm^2$ in rectangle) were cleaned by sonication in acetone, deionized water, and ethanol for 15 min each and heated at 500 °C for 2 h. In details, $1.25 \times 10^{-3}$M Nickel nitrate, $2.5 \times 10^{-3}$M Cobalt nitrate and $3.75 \times 10^{-3}$M citric acid was dissolved in 50 ml pure $H_2O$ under vigorous stirring, resulting in light pink solution. The cleaned carbon cloth was soaked in 0.2 ml of this pink solution and then placed in an electrical oven previously designated at 70 °C for drying. After 2 h, the as-obtained precursor was further calcined in a tubular furnace at 300 °C for 2 h in air. After being slowly cooled down to room temperature, sample NC@C appeared. $NiCo_2O_4$@carbon cloth without citric acid (NC1@C) was prepared to compare with NC@C

### 2.2 Characterization

The structures and morphologies of as-synthesized samples were characterized by X-ray power diffraction (XRD, Rigaku D/MAX 2500, Cu Kα radiation), scanning electron microscope (SEM, FEI Nova Nano-SEM 230) and transmission electron microscope (TEM, JEOL JEM-2100F). The NC@C was direct used as working electrode without any binder. The NC@C was cut into sheets of $1 \times 1$ $cm^2$. The amount of active materials on the carbon cloth was obtained by weighing the mass of the carbon cloth (treated via the anneal of 500 °C for 2 h) and the prepared sample in a high-precision analytical balance. Each electrode contains about 0.6 mg of electroactive materials, which is the same to the amount growing on carbon cloth using hydrothermal method.

### 2.3 Electrochemical measurements

The electrochemical performance was evaluated by using three-electrode system with Pt foil as counter electrode and

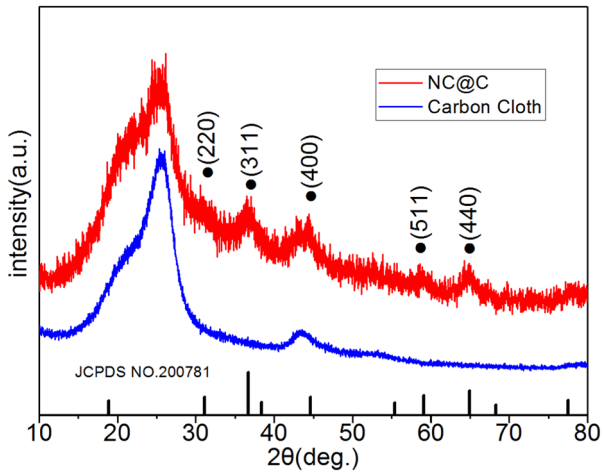


**Fig. 1** XRD patterns of NC@C and carbon cloth

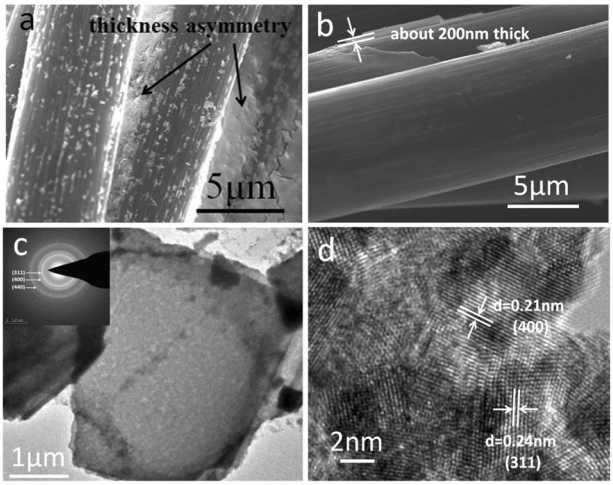


**Fig. 2** **a** SEM images of the NC1@C; **b** SEM images of the NC@C; **c** TEM images of NC@C and inset shows the SAED pattern; **d** HRTEM image of the NC@C

Hg/HgO (KOH, $a = 1$) as reference electrode in 2 M KOH aqueous solution. The electrochemical measurements were carried out by using electrochemical workstation (CHI660E, Shanghai). To observe the pair of symmetrical and reversible redox peaks in high scan rates and ensure high Coulombic efficiency in even low current density testing, we measured cyclic voltammograms (CV) in the voltage range of 0−0.55 V (vs. Hg/HgO) at various scan rates, and galvanostatic charge-discharge (GCD) tests were measured in the voltage range of 0−0.52 V (vs. Hg/HgO) under different current densities.

## 3 Results and discussion

### 3.1 Physicochemical characterization

The crystalline structure and phase purity of the samples were characterized by XRD. All the diffraction peaks ((220), (311), (400), (511), and (440)) in Fig. 1 can be indexed to the spinel $NiCo_2O_4$ crystalline structure (JCPDS No: 20-0781) and no other peaks were found, except a broad peak arising from the CF substrate at 20–30 degree. The relatively broad peaks of $NiCo_2O_4$ reveal the small crystallite size or low crystallinity [27, 28].

The morphology of NC1@C is illustrated in Fig. 2a. According to the scanning electron microscopy (SEM) image, carbon fibers with rough surface could be observed, indicating the $NiCo_2O_4$ nanolayer not uniformly covered on the surface of carbon nanofibers. The morphology of NC@C is illustrated in Fig. 2b. According to the SEM image, carbon fibers with smooth surface could be observed, indicating the $NiCo_2O_4$ nanolayer uniformly covered on the surface of carbon nanofibers. The coating thickness is about 200 nm. The selected-area diffraction (SAED) pattern for NC@C (Fig. 2c inset)indicates high crystallinity, and each diffraction ring is also well indexed to $NiCo_2O_4$. Figure. 2d shows high-resolution TEM image of the NC@C, in which an interplanar spacing of 0.24 nm and 0.21 nm is assigned to the (311) and (400) lattice plane of NiCo2O4, respectively [29–34].

### 3.2 Electrochemical characterization

To evaluate the potential of the as-synthesized NC@C acting as an electrode material for high rate supercapacitor, the electrochemical capacitive behavior was elucidated by the CV method. Figure 3a depicts representative CV curves measured at various scan rates ranging from 1 to 30 mV $s^{-1}$ in a potential range of 0.0−0.55 V (vs. Hg/HgO) in 2.0 M KOH solution. The redox peaks are observed in anodic and cathodic sweeps in all CV curves, illustrating that the electrochemical capacitance of the NC@C is mainly based on the redox mechanism. The redox peaks are mainly attributed to the redox reactions related to Ni−O/Ni−O−OH or Co−O/Co−O−OH. there is only one couple of redox peaks of $Ni^{2+}/Ni^{3+}$ and $Co^{2+}/Co^{3+}$, due to the similar redox potential of $Co_3O_4$ and NiO, the structure of the NC@C which can induce appreciable broadening of some redox peaks. the peak of the CV curves current increase with increasing scan rates. Also, the shape of the CV curves is not obviously changed by increasing the scan rate indicating the good kinetic reversibility of the NC@C electrodes. It is evident that the D-value of redox peaks grows in size with the scan rates increasing, respectively. When the scan rate is 5 mV $s^{-1}$, the redox peaks are around 0.33 and 0.44 V. When the scan rate is 100 mV $s^{-1}$, the redox peaks are extended to 0.27 and 0.48 V. the cathodic peak shifts

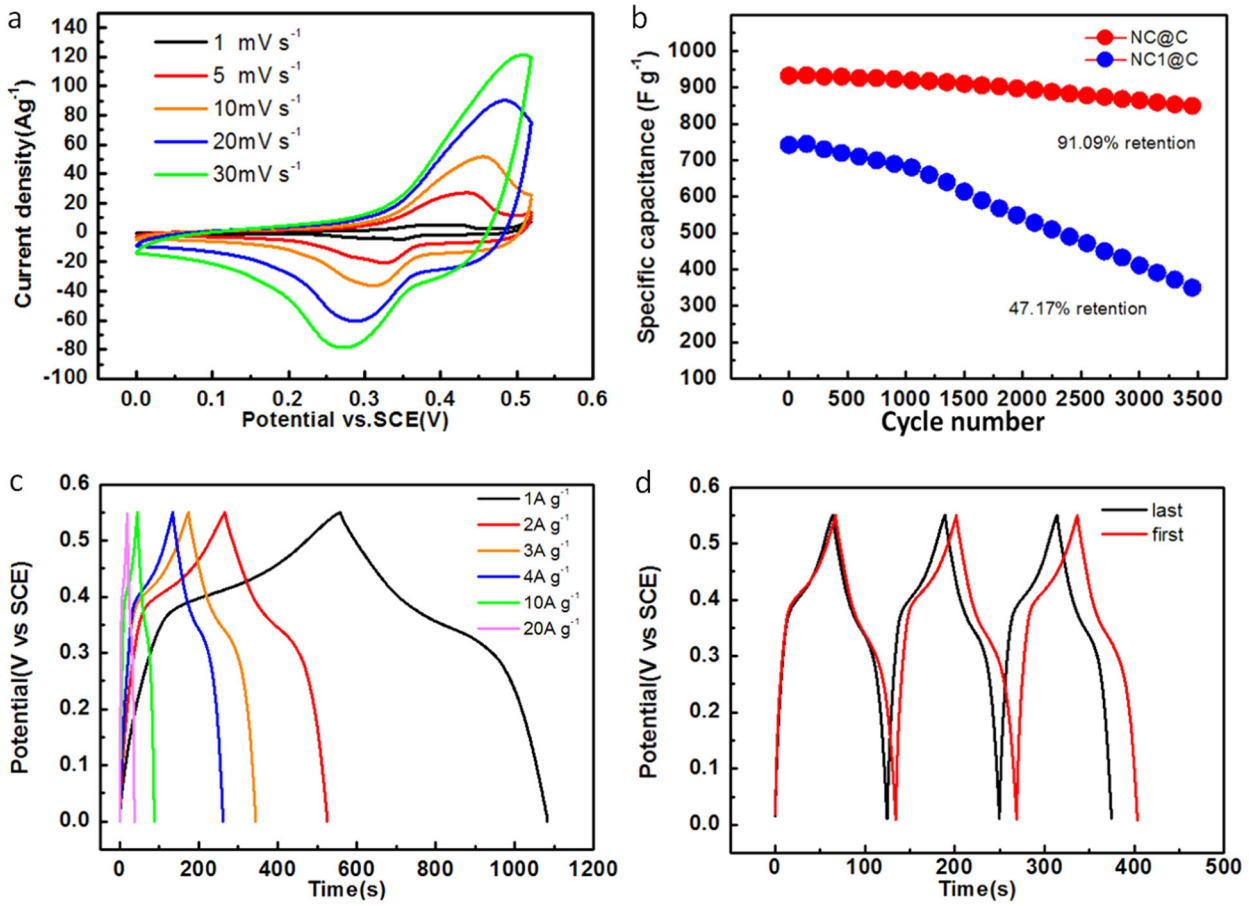


**Fig. 3** **a** Electrochemical properties of the NC@C: **b** Cycle performance of the NC@C electrode and the NC1@C electrode for 3500 successive charge−discharge cycles at a current density of 1 A g$^{-1}$. **c** galvanostatic charge−discharge(GCD) curves of the NC@C electrode at different current densities. **d** the first and the last three GCD cycles of 3500-cycling test at 1 A g$^{-1}$

slightly from 0.33 to 0.27 V. This observation suggests a relatively low resistance of the electrode because of the good contact between the electroactive $NiCo_2O_4$ nanolayer and the conductive carbon clothe substrate.

The cycling stability of the NC@C and the NC1@Cwas also evaluated by the repeated charging/discharging measurement at a constant current density of 1 mA cm$^{-2}$, as shown in Fig. 3d. Specific capacity (SC) can be determined by following equation:

$$SC = \frac{i\Delta t}{m\Delta V}$$

Where SC, i, Δt, m, andΔV are specific capacity (C/g), current (A), discharge time (s), the mass (g) of active materials, and the potential window (V), respectively. When a discharge current density of 1 mA cm$^{-1}$ is applied, the specific capacity of NC@C electrode reaches a high value of 944.5 F g$^{-1}$ and it gradually decreases to 859.5 F g$^{-1}$ over 3500 cycles, resulting in an overall capacitance loss of only 8.9%. The capacity and stability of NC1@C is not the same as NC@C. The specific capacity of NC1@C electrode is just 748.5 F g$^{-1}$ and it rapidly decreases to 353.0 F/g over 3500 cycles, resulting in an overall capacitance loss of 52.8%. Considering the morphologies of NC@C and NC1@C illustrated in Fig. 2, it is easy to illuminate why the capacity and stability of NC1@C electrode lower than NC@C electrode. On the NC1@C electrode, the $NiCo_2O_4$ active material is asymmetry and likely to fall off. On the NC@C electrode, the $NiCo_2O_4$ active material is homogeneous and closely combined with carbon cloth. Figure. 3c shows the galvanostatic discharge curves of as-synthesized NC@C testing under different current densities within the potential range from 0 to 0.55 V (vs. Hg/HgO). With the increase of discharge current densities, a larger voltage drop can be observed in Fig. 3c, leading to the decrease of capacitance in high-rate. It can be observed that there are voltage plateaus between 0.30 and 0.41 V, which is consistent with observations in previous reports in the literature. Figure. 3d shows the first three and the last three GCD cycles of the 3500-cycling test at a current density

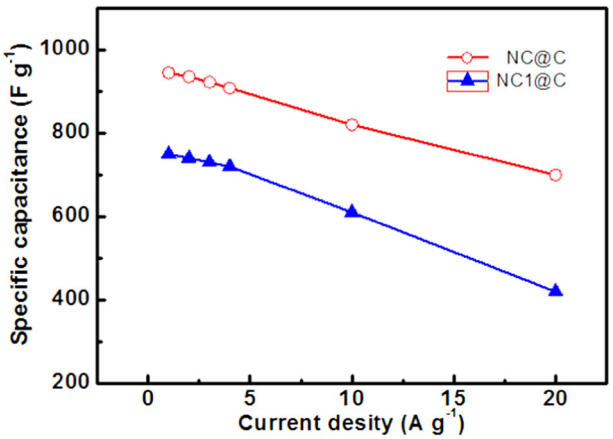


**Fig. 4** The specific capacitance of the NC@C electrode and the NC1@C electrode at various current densities

of 1 A $g^{-1}$. The charge−discharge plateaus of the last three cycles turn into shorter than that of the beginning, resulting in a capacitance decrease.

The corresponding plot of discharge capacitance versus current density of NC@C electrode is shown in Fig. 4, along with the comparative data of NC1@C electrode. The NC@C electrode can deliver a high specific capacitance of 944.5 F $g^{-1}$ at a current density of 1 A $g^{-1}$ and a specific capacitance of 702.4 F $g^{-1}$ is still retained at a very high current density of 20 A $g^{-1}$, which are much higher than the NC1@C electrode at the same current densities.

## 4 Conclusions

In conclusion, we have successfully synthesize an ultrathin $NiCo_2O_4$ nanolayer on flexible carbon cloth with strong adhesion for high-performance supercapacitors. $NiCo_2O_4$ nanolayer covered on surface of the carbon cloth is synthesized by a one-step route which is only involved a modified sol–gel method. The binder-free electrode only with simple layer covering on carbon cloth displays outstanding pseudocapacitive behaviors in 2 M KOH, which exhibits high specific capacitances of 944.5 F $g^{-1}$ at 1 A $g^{-1}$ and 702.4 F $g^{-1}$ at 20 A $g^{-1}$after activation, as well as excellent cycling stability. The specific capacitance can still retain 859.5 F $g^{-1}$ (91% retention) at a current density of 1 A $g^{-1}$ after 3500 cycles.

**Acknowledgements** This work is supported by the National Natural Science Foundation of China (grant Nos. 51472271, 51772331).

### Compliance with ethical standards

**Conflict of interest** The authors declare that they have no conflict of interest.

## References

1. Yang Q, Wu J, Huang K, Lei M, Wang W, Tang S, Liu J (2016) Layer-by-layer self-assembly of graphene-like $Co_3O_4$ nanosheet/graphene hybrids: Towards high-performance anode materials for lithium-ion batteries. J Alloy Compd 667:29–35
2. Yang L, Li H, Liu J, Lu Y, Li S, Min J, Lei M (2016) Effects of $TiO_2$ phase on the performance of $Li_4Ti_5O_{12}$ anode for lithium-ion batteries. J Alloy Compd 689:812–819
3. Zhu K, Liu J, Li S, Liu L, Yang L, Liu S, Xie T (2017) Ultrafine cobalt phosphide nanoparticles embedded in nitrogen-doped carbon matrix as a superior anode material for lithium ion batteries. Adv Mater Interfaces 4(19):1–8
4. Lu YB, Wu JB, Liu JB, Lei M, Tang SB, Lu PB, Yang QB (2015) Facile synthesis of $Na_{0.33}V_2O_5$ nanosheet-graphene hybrids as ultrahigh performance cathode materials for lithium ion batteries. ACS Appl Mater Interfaces 7(31):17433–17440
5. Liu S, Zhou J, Cai Z, Fang G, Cai Y, Pan A, Liang S (2016) $Nb_2O_5$ quantum dots embedded in MOF derived nitrogen-doped porous carbon for advanced hybrid supercapacitors applications. J Mater Chem A 4:17838–17847
6. Yu D, Yao J, Qiu L, Wang Y, Zhang X, Feng Y, Wang H (2014) In situ growth of $Co_3O_4$ nanoparticles on α-$MnO_2$ nanotubes: a new hybrid for high-performance supercapacitors. J Mater Chem A 2(22):8465
7. Hasegawa G, Kanamori K, Kiyomura T, Kurata H, Abe T, Nakanishi K (2016) Hierarchically porous carbon monoliths comprising ordered mesoporous nanorod assemblies for high-voltage aqueous supercapacitors. Chem Mater 28(11):3944–3950
8. Wang F, Xiao S, Hou Y, Hu C, Liu L, Wu Y (2013) Electrode materials for aqueous asymmetric supercapacitors. RSC Adv 3 (32):13059
9. Nguyen VH, Shim JJ (2015) In situ growth of hierarchical mesoporous $NiCo_2S_4$@$MnO_2$ arrays on nickel foam for high-performance supercapacitors. Electrochim Acta 166:302–309
10. Dong L, Xu C, Li Y, Huang ZH, Kang F, Yang QH, Gencer Imer A (2016) All-solid-state high performance asymmetric supercapacitors based on novel MnS nanocrystal and activated carbon materials. Sci Rep 6:23289
11. Jabeen N, Hussain A, Xia Q, Sun S, Zhu J, Xia H (2017) High-performance 2.6 V aqueous asymmetric supercapacitors based on in situ formed $Na_{0.5}MnO_2$ nanosheet assembled nanowall arrays Adv Mater 29(32):1700804
12. Wang P, Zhao Y-J, Wen L-X, Chen J-F, Lei Z-G (2014) Ultrasound–microwave-assisted synthesis of $MnO_2$ supercapacitor electrode materials. Ind Eng Chem Res 53:20116–20123
13. Senthilkumar ST, Fu N, Liu Y, Wang Y, Zhou L, Huang H (2016) Flexible fiber hybrid supercapacitor with $NiCo_2O_4$ nanograss@carbon fiber and bio-waste derived high surface area porous carbon. Electrochim Acta 211:411–419
14. Wang L, Jiao X, Liu P, Ouyang Y, Xia X, Lei W, Hao Q (2018) Self-template synthesis of yolk-shelled $NiCo_2O_4$ spheres for enhanced hybrid supercapacitors. Appl Surf Sci 427:174–181
15. Godillot G, Taberna P-L, Daffos B, Simon P, Delmas C, Guerlou-Demourgues L (2016) High power density aqueous hybrid supercapacitor combining activated carbon and highly conductive spinel cobalt oxide. J Power Sources 331:277–284
16. Wu C, Lu X, Peng L, Xu K, Peng X, Huang J, Xie Y (2013) Two-dimensional vanadyl phosphate ultrathin nanosheets for high energy density and flexible pseudocapacitors. Nat Commun 4:2431
17. Huang Z, Zhang Z, Qi X, Ren X, Xu G, Wan P, Zhang H (2016) Wall-like hierarchical metal oxide nanosheet arrays grown on carbon cloth for excellent supercapacitor electrodes. Nanoscale 8 (27):13273–13279

18. Xiao X, Ding T, Yuan L, Shen Y, Zhong Q, Zhang X, Wang ZL (2012) WO 3-x/MoO3-x core/shell nanowires on carbon fabric as an anode for all-solid-state asymmetric supercapacitors. Adv Energy Mater 2(11):1328–1332
19. Min J, Liu J, Lei M, Wang W, Lu Y, Yang L, Su N (2016) Self-assembly of parallelly aligned NiO hierarchical nanostructures withultrathin nanosheet subunits for electrochemical supercapacitor applications. ACS Appl Mater Interfaces 8(1):780–791
20. Heydari H, Gholivand MB (2017) Novel synthesis and characterization of $ZnCo_2O_4$ nanoflakes grown on nickel foam as efficient electrode materials for electrochemical supercapacitors Ionics 23(6):1489–1498
21. Niu H, Yang X, Jiang H, Zhou D, Li X, Zhang T, Qu F (2015) Hierarchical core–shell heterostructure of porous carbon nanofiber@$ZnCo_2O_4$ nanoneedle arrays: advanced binder-free electrodes for all-solid-state supercapacitors. J Mater Chem A 00:1–13
22. Li S, Liu G, Liu J, Lu Y, Yang Q, Yang L-Y, Han M (2016) Carbon fiber cloth@$VO_2$ (B): Excellent binder-free flexible electrodes with ultrahigh mass-loading. J Mater Chem A 4(17):6426–6432
23. Luo Y, Zhang H, Wang L, Zhang M, Wang T (2015) Fixing graphene-$Mn_3O_4$ nanosheets on carbon cloth by a poles repel-assisted method to prepare flexible binder-free electrodes for supercapacitors. Electrochim Acta 180:983–989
24. Peng T, Yi H, Sun P, Jing Y, Wang R, Wang H, Wang X (2016) In situ growth of binder-free CNTs@Ni–Co–S nanosheets core/shell hybrids on Ni mesh for high energy density asymmetric supercapacitors. J Mater Chem A 4(22):8888–8897
25. Xia H, Xia Q, Lin B, Zhu J, Seo JK, Meng YS (2016) Self-standing porous $LiMn_2O_4$ nanowall arrays as promising cathodes for advanced 3D microbatteries and flexible lithium-ion batteries. Nano Energy 22:475–482
26. Zhang G, Lou XW (2013) General solution growth of mesoporous $NiCo_2O_4$ nanosheets on various conductive substrates as high-performance electrodes for supercapacitors. Adv Mater 25 (7):976–979
27. Du J, Zhou G, Zhang H, Cheng C, Ma J, Wei W, Wang T (2013) Ultrathin porous $NiCo_2O_4$ nanosheet arrays on flexible carbon fabric for high-performance supercapacitors. ACS Appl Mater Interfaces 5(15):7405–7409
28. Gao G, Wu H, Bin, Ding S, Liu LM, Lou XW (2015) Hierarchical $NiCo_2O_4$ nanosheets grown on Ni nanofoam as high-performance electrodes for supercapacitors. Small 11(7):804–808
29. Zhao L, Wang L, Yu P, Tian C, Feng H, Diao Z, Fu H (2017) Hierarchical porous $NiCo_2O_4$ nanosheet arrays direct grown on carbon cloth with superior lithium storage performance Dalton Trans 46(14):4717
30. Jabeen N, Xia Q, Yang M, Xia H (2016) Unique core-shell nanorod arrays with polyaniline deposited into mesoporous $NiCo_2O_4$support for high-performance supercapacitor electrodes. ACS Appl Mater Interfaces 8(9):6093–6100
31. Wu YQ, Chen XY, Ji PT, Zhou QQ (2011) Sol-gel approach for controllable synthesis and electrochemical properties of $NiCo_2O_4$ crystals as electrode materials for application in supercapacitors. Electrochim Acta 56(22):7517–7522
32. Liu X, Shi S, Xiong Q, Li L, Zhang Y, Tang H, Tu J (2013) Hierarchical $NiCo_2O_4$ @ $NiCo_2O_4$ core/shell nanoflake arrays as high-performance supercapacitor materials. ACS Applied. Mater Interfaces 5(17):8790–8795
33. Shen L, Yu L, Yu XY, Zhang X, Lou XWD (2015) Self-templated formation of uniform $NiCo_2O_4$ hollow spheres with complex interior structures for lithium-Ion batteries and supercapacitors. Angew Chem-Int Ed 54(6):1868–1872
34. Tong X, Chen S, Guo C, Xia X, Guo X-Y (2016) Mesoporous $NiCo_2O_4$ nanoplates on three-dimensional graphene foam as an efficient electrocatalyst for the oxygen reduction reaction. ACS Appl Mater Interfaces 5:b10044